

TractCaliber: Axon diameter estimation across white matter tracts in the *in vivo* human brain using 300 mT/m gradients

Susie Y. Huang¹, Thomas Witzel¹, Qiuyun Fan¹, Jennifer A. McNab², Lawrence L. Wald^{1,3}, and Aapo Nummenmaa¹

¹Athinoula A. Martinos Center for Biomedical Imaging, Department of Radiology, Massachusetts General Hospital, Charlestown, MA, United States, ²Radiological Sciences Laboratory, Department of Radiology, Stanford University, Stanford, CA, United States, ³Harvard-MIT Division of Health Sciences and Technology, Massachusetts Institute of Technology, Cambridge, MA, United States

PURPOSE: Diffusion tractography provides a noninvasive tool for mapping the major white matter pathways of the human brain *in vivo*.¹ The ability of fiber-tracking to elicit accurate measures of structural connectivity may be augmented by incorporating quantitative microstructural information on the size of axons, particularly in regions where fibers are expected to cross.²⁻⁴ The advent of higher maximum gradient strengths on human MRI scanners⁵ has enabled the translation of AxCaliber,^{3,7,8} ActiveAx,^{2,9} and other axon diameter mapping methods from small animal⁸ and ex vivo studies^{3,7} to the *in vivo* human brain.^{2,9,11,12} Higher gradient strengths offer more accurate estimates of axon diameter¹² and improved resolution of fiber crossings.¹³ In this work, we use a novel 3 T MRI equipped with 300 mT/m gradients to obtain tract-specific measures of axon diameter for fibers of any orientation in the *in vivo* human brain. Our approach provides consistent estimates of axon diameter across the corpus callosum (CC) and corticospinal tracts (CST), similar to those reported by histology.

METHODS: Data acquisition. A healthy volunteer was scanned on a dedicated high-gradient 3 T MRI scanner (MAGNETOM CONNECTOM, Siemens Healthcare) with maximum gradient strength of 300 mT/m and maximum slew rate of 200 mT/m/ms using a custom-made 64-channel phased array head coil.⁵ Sagittal 1.5-mm isotropic resolution diffusion-weighted spin echo EPI were acquired with 93 contiguous slices using simultaneous multislice (SMS) imaging⁵ and zoomed/ parallel imaging⁶ for high-resolution whole-brain coverage. The following parameters were used: $\delta=8$ ms, $\Delta=19/36/56$ ms, 8 diffusion gradient increments linearly spaced from 25–293 mT/m per Δ for a total of 24 q -shells, TE/TR=83/3600 ms, GRAPPA acceleration factor R=2, and SMS MB factor=3. Diffusion gradients were applied in 64 non-collinear directions with 5 interspersed $b=0$ images. The maximum b -value at the longest diffusion time was 20,550 s/mm². Total acquisition time was 103 min.

Data analysis. The data was preprocessed to correct for distortions due to gradient nonlinearity, motion and eddy currents.¹³ Generalized q -sampling imaging (GQI) was used to combine the q -shell data for the highest SNR diffusion time ($\Delta=19$ ms) and determine the principal fiber direction in each voxel. Spherical harmonics expansion of order 6 with Laplace-Beltrami regularization¹⁴ was then used to interpolate the data to determine the average signal perpendicular to the principal fiber direction. The regularization parameter λ was set to 0.006.

A three-compartment model of intra-axonal, extra-axonal, and free diffusion was fitted to the data to obtain estimates of axon diameter, restricted and free diffusion volume fractions, and hindered diffusivity,¹² fitting for a single axon diameter as in ActiveAx.^{2,9} A Markov chain Monte Carlo simulation provided samples of the posterior distributions of the model parameters given the data using broad uniform priors. From the GQI data set, fiber tracking was performed with DSI Studio¹⁵ using standard deterministic fiber tracking.

RESULTS: Maps of mean axon diameter and restricted fraction in the midline sagittal CC showed larger diameter axons and decreased restricted fraction in the body (Fig. 1a and b). This trend was also reflected in ROI analysis of axon diameter in different regions of the midline sagittal CC, which showed a low-high-low pattern of axon diameter from anterior to posterior, in agreement with known trends from histology.¹⁶ Furthermore, estimates of mean axon diameter were consistent across the major white matter tracts, including the CC and CST (Fig. 2). The axon diameters in the CST and body of the CC were larger (~6–7 μ m) compared to the surrounding white matter tracts, in keeping with histologic observations.^{16,17} Figure 3 shows local estimates of axon diameter along the CSTs and histograms of axon diameters demonstrating similar estimates of mean axon diameter and distribution in the bilateral CSTs.

DISCUSSION: TractCaliber leverages cutting-edge techniques for accelerating slice and in-plane image acquisition to achieve 1.5 mm³ isotropic resolution throughout the whole brain. We adopt a simple yet powerful analysis method to estimate tract-specific axon diameters through combining GQI and modeling of intra- and extra-axonal compartments. The relatively constant axon diameter estimates along the CC and CST agree with histological observations that axon diameters do not vary considerably along any given axonal projection.¹⁶ The larger axon diameters seen in the body of the CC and CST are also in agreement with known histological trends. Future work will focus on optimizing the acquisition protocol and expanding the model to account for orientation dispersion² and fiber crossings,³ which may further refine axon diameter estimates along the tracts.

CONCLUSION: We present the first demonstration of axon diameter estimation across fiber bundles of arbitrary orientation in the *in vivo* human brain using gradient strengths up to 300 mT/m. The agreement of our results with histological observations supports the use of high gradient strengths for accurate estimation of axon diameters across white matter tracts *in vivo*.

REFERENCES: [1] Catani M et al. *NI* 17:77 (2002). [2] Zhang H et al. *NI* 56:1301 (2011). [3] Barazany D et al., *Proc ISMRM* 19:76 (2011). [4] Assaf Y et al. *NI* 80:273 (2013). [5] Setsompop K et al. *NI* 80:220 (2013). [6] Eichner C et al. *MRM* 71:1518 (2014). [7] Assaf Y et al. *MRM* 59:1347 (2008). [8] Barazany D et al. *Brain* 132:1210 (2009). [9] Alexander DC et al. *NI* 52:1374 (2010). [10] Stanisz GJ et al. *MRM* 37:103 (1997). [11] McNab JA et al. *NI* 80:234 (2013). [12] Huang SY et al. *Proc ISMRM* 22:6386 (2014). [13] Fan Q et al. *Brain Connectivity* doi:10.1089/brain.2014.0305 (2014). [14] Descoteaux M et al. *MRM* 58:497 (2007). [15] <http://dsi-studio.labsolver.org/> [16] Aboitiz F et al. *Brain Res* 598:143 (1992). [17] Graft et al. *Anat Anz* 157:97 (1984). [18] Perge JA et al. *J Neuroscience* 29:7917 (2009).

ACKNOWLEDGMENTS: Supported by NIH U01MH093765, NCR P41EB015896, NIBIB K99EB015445, and an RSNA Resident Research Grant.

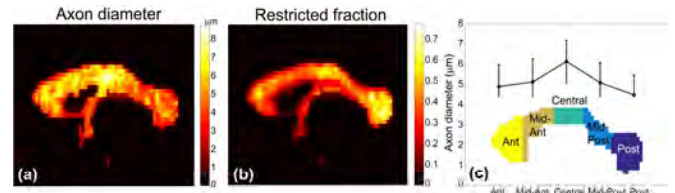


Figure 1: Maps of (a) mean axon diameter and (b) restricted fraction, and (c) ROI analysis of axon diameter estimates in the midline sagittal corpus callosum.

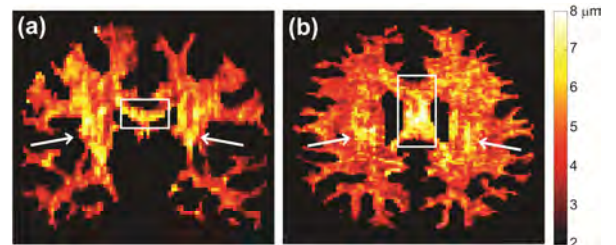


Figure 2: Voxel-wise estimates of mean axon diameter from (a) coronal slice through the level of the precentral gyrus (curved arrows) and (b) axial slice through the body of the corpus callosum showing consistently larger axon diameters in the corticospinal tracts (arrows) and corpus callosum (rectangle).

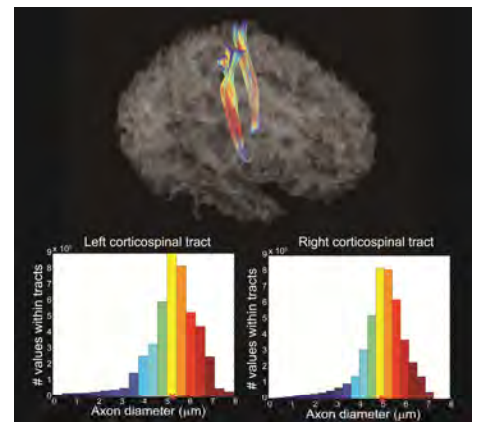


Figure 3: (Top) Local estimates of axon diameter along the corticospinal tracts. (Bottom) Histograms of axon diameter in the left and right corticospinal tracts, with the mean axon diameter for each histogram denoted with an x.